# Dry-Contact Electrode Ear-EEG

Simon L. Kappel, *Member, IEEE*, Mike L. Rank, *Member, IEEE*, Hans Olaf Toft, Mikael Andersen, and Preben Kidmose, *Senior Member, IEEE*

***Abstract*—*Objective:*** **Ear-EEG is a recording method in which EEG signals are acquired from electrodes placed on an earpiece inserted into the ear. Thereby, ear-EEG provides a noninvasive and discreet way of recording EEG, and has the potential to be used for long-term brain monitoring in real-life environments. Whereas previously reported ear-EEG recordings have been performed with wet electrodes, the objective of this study was to develop and evaluate dry-contact electrode ear-EEG.** ***Methods:*** **To achieve a well-functioning dry-contact interface, a new ear-EEG platform was developed. The platform comprised actively shielded and nanostructured electrodes embedded in an individualized soft-earpiece. The platform was evaluated in a study of 12 subjects and four EEG paradigms: auditory steady-state response, steady-state visual evoked potential, mismatch negativity, and alpha-band modulation.** ***Results:*** **Recordings from the prototyped dry-contact ear-EEG platform were compared to conventional scalp EEG recordings. When all electrodes were referenced to a common scalp electrode (Cz), the performance was on par with scalp EEG measured close to the ear. With both the measuring electrode and the reference electrode located within the ear, statistically significant ($p < 0.05$) responses were measured for all paradigms, although for mismatch negativity, it was necessary to use a reference located in the opposite ear, to obtain a statistically significant response.** ***Conclusion:*** **The study demonstrated that dry-contact electrode ear-EEG is a feasible technology for EEG recording.** ***Significance:*** **The prototyped dry-contact ear-EEG platform represents an important technological advancement of the method in terms of user-friendliness, because it eliminates the need for gel in the electrode-skin interface.**

***Index Terms*—Electroencephalography (EEG), ear-EEG, dry-contact biopotential electrode, iridium oxide, wearable EEG.**

## I. Introduction

FOR decades, researchers and clinicians have been interested in measuring EEG outside the laboratory. In recent years, this interest have gained momentum due to significant technological advancements of wearable devices, and demands for better and more efficient health care technology. Ambulatory EEG systems exist and enable long-term real-life recordings, but they are typically bulky and obtrusive for the users everyday life activities, and must be mounted by trained personnel [1]. Wearable EEG systems try to overcome the limitations of ambulatory systems, aiming at user friendly systems which are easy to mount and which enable long-term recordings in the everyday life. Moreover, the development of some wearable EEG systems have also focused on designs that are both discreet in use and unobtrusive during everyday life activities [2]–[5].

Conventional laboratory EEG recordings are performed with full cap systems and wet electrodes to obtain high quality measurements with high spatial resolution. In contrast, wearable EEG systems typically have lower spatial resolution, and dry-contact electrodes are used to improve the user-friendliness and feasibility for long-term recordings.

When using dry-contact electrodes, no electrode gel is applied between the electrodes and the skin, instead the instrumentation and electrodes are designed to accommodate and reduce the effect of variations in the electrode-skin interface [6], [7]. Dry-contact electrodes have been proposed in various designs, including mesh electrodes laminated onto the skin [4], flexible polymer based electrodes [3], [8], [9], and spring loaded electrodes [10], [11].

Ear-EEG is a method in which EEG is recorded from electrodes in the outer ear [12]–[14]. Ear-EEG addresses the practical challenges of non-invasive and robust EEG acquisition in real-life environments. The shape of ear-EEG devices are very similar to the earpieces used for hearing aids and provides a discreet and comfortable way of recording EEG. Thus, wearable EEG systems based on ear-EEG could be used to perform continuous EEG monitoring for several days.

Previous ear-EEG recordings have been performed with wet electrodes, in which conductive gel was applied between the electrodes and the skin [12], [14], [15]. Dry-contact electrode ear-EEG would increase the comfort and user-friendliness of ear-EEG devices, and would enable the user to insert the device without assistance. In addition, the skin preparation, typically needed for wet ear-electrodes, could be avoided [6].

This paper presents a novel dry-contact ear-EEG platform, comprising dry-contact electrodes and a soft-earpiece. The electrode and earpiece design were validated through a study of standard EEG paradigms. Recordings performed with the dry-contact ear-EEG platform were compared to standard wet electrode scalp EEG recordings.

The study was approved by the regional scientific ethics committee (case no: 1-10-72-46-17).

Manuscript received December 19, 2017; revised February 11, 2018 and April 5, 2018; accepted May 5, 2018. Date of publication May 11, 2018; date of current version December 19, 2018. This work was supported by Innovation Fund Denmark (j.nr. 110-2013-1). *(Corresponding author: Simon L. Kappel.)*

S. L. Kappel is with Department of Engineering, Aarhus University, DK-8200 Aarhus, Denmark (e-mail: slk@eng.au.dk).

M. L. Rank, H. O. Toft, and M. Andersen are with UNEEG Medical A/S. P. Kidmose is with the Department of Engineering, Aarhus University.

Digital Object Identifier 10.1109/TBME.2018.2835778

## II. Methods

This section is divided into four main parts. The first part (Sections II-A and II-B) describes the novel dry-contact ear-EEG platform. The second part (Sections II-C and II-D) describes the experimental setup and the electrode configurations used in the data analysis. The third part (Sections II-E, II-F, II-G, and II-H) describes the experimental paradigms and signal processing methods used to assess the quality of the recorded EEG signals. And finally, the fourth part (Section II-I and II-J) describes evaluation methods for characterization of the electrode-skin impedance and half-cell potential.

### A. Dry-Contact Ear-EEG Electrodes

Recording of bioelectrical signals from electrodes placed on the surface of the skin relies critically on the electrode-skin interface. For dry-contact electrodes this interface is mainly defined by the electrochemical properties of the electrode material, the mechanical design of the electrode, the surface properties of the electrode, and how the electrode is retained against the skin. Thus, a good dry-contact electrode interface for ear-EEG relies both on the electrode itself and how it is mounted in the ear. This subsection describes the developed electrode, and the following subsection describes the soft-earpieces used for the electrodes.

The electrode was based on a titanium (Ti) substrate coated with iridium-oxide ($IrO_2$) and mechanically designed to be embedded into a soft-earpiece. $IrO_2$ is a well characterized material with pseudocapacitive properties and low impedance. $IrO_2$ coatings have previously been used for both tissue stimulation [16], [17] and measuring biopotentials [18].

The $IrO_2$ coating for the current study was a thermal iridium oxide film (TIROF) formed on an etched Ti surface [19], [20]. The electrode was evaluated biocompatible[1] by UL (2017, Germany), according to the EN ISO 10993-1 standards. The coating was mechanically robust and highly inert, thus suitable for long-term skin contact during recordings in the everyday life. In addition, the coating had hydrofilic properties, causing it to easily become moist, when applied to the skin.

The electrode assembly was based on a circular $IrO_2$ coated Ti-pin, which was electrically shielded by a housing made of silver (Ag). The Ti-pin and the shielding house was electrically isolated by a spacer made of polymer, as shown in Fig. 1. The core of a coax cable was connected to the Ti-pin, and the shield of the cable was connected to the housing. Epoxy adhesive was applied on the backside of the construction, as illustrated in Fig. 1.

The electrode was designed to be inserted into holes in a soft-earpiece, as shown in Fig. 2(a) and (b). Previous ear-EEG earpieces have been constructed of rigid acrylic plastic with electrodes made of silver epoxy painted onto the surface of the earpiece. Thus, the electrodes could not be reused for another earpiece. The designed $IrO_2$ electrode is generic and can be moved from one earpiece to another.

[1]The electrode was testet for cytotoxicity, irritation, and delayed type of hypersensitivity without remarks. In addition, gas chromatographic fingerprint investigations and inductively coupled plasma (ICP-EOS) investigation were performed to investigate leachable substances from the electrode. Both investigations evaluated the leachable substances from the electrode to be uncritical.

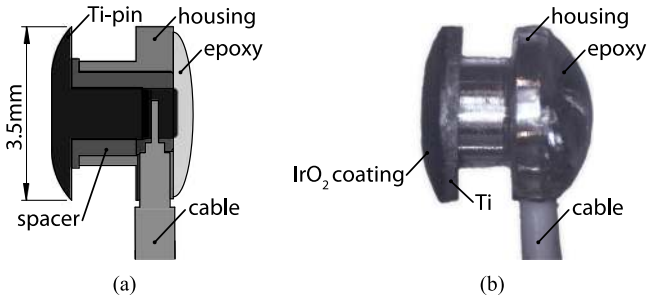


Fig. 1. (a) Cross sectional sketch of the dry-contact $IrO_2$ electrode design. (b) Microscope picture of the designed electrode.

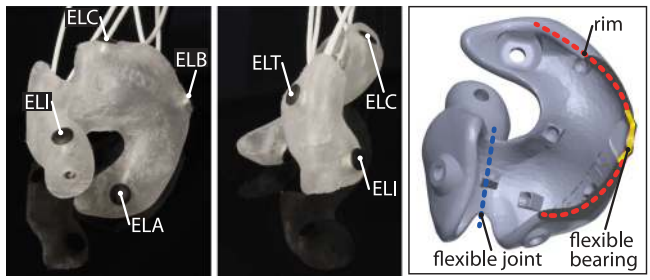


Fig. 2. (a) and (b) Soft-earpiece for the left ear, with electrodes inserted in positions A, B, C, T, E, and I. (c) Sketch of an earpiece, with indication of the methods used to improve skin contact for dry-contact electrode recordings.

### B. Soft-Earpieces

To obtain a firm electrode-skin contact, we found it to be of crucial importance to have the developed electrode mounted in a soft-earpiece customized to the anatomical shape of the individual ear. This was particularly important to achieve a good and reliable contact with the skin in the concha part of the ear. The flexibility of the earpiece allowed it to follow changes in the shape of the ear, and helped the electrodes to maintain a stable contact with the skin during these changes. For the current study, electrode holes were created in positions ExA, ExB and ExC in the concha part of the outer ear, and positions ExE, ExI and ExT in the ear-canal, where x denotes the left (L) or right (R) ear [12]. The ExT electrode was facing the tragus of the ear. Fig. 2(a) and (b) show the position of the electrodes on an earpiece.

Earpieces for the study were designed with a flexible joint between the ear-canal and the concha part of the earpiece, as shown in Fig. 2(c). This enabled the ear-canal and concha part of the earpiece to move independently, facilitating less motion of the electrodes during e.g., jaw movements [21]. The ExT electrode and the electrodes located in concha were mounted in flexible bearings elevated towards the skin, creating an increased skin pressure at the location of the electrode. The electrodes located in the concha are especially prone to lose skin contact [6]. Therefore, the concha electrodes were located at the rim of the earpiece, where the C-shape between concha cymba and anti tragus helped to create pressure towards the skin. The earpieces were made of biocompatible elastic earmould silicone (Detax Softwear 2.0, Shore A 60).

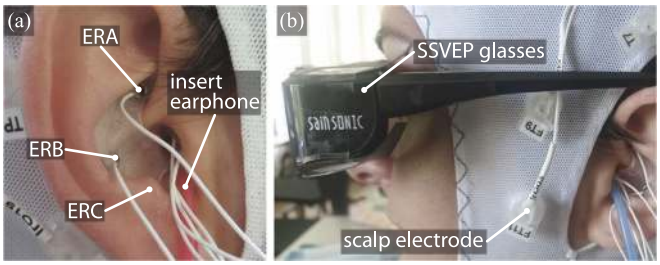


Fig. 3. (a) An earpiece and insert earphone mounted in the ear. (b) A subject wearing SSVEP glasses and the cap with $IrO_2$ scalp electrodes.

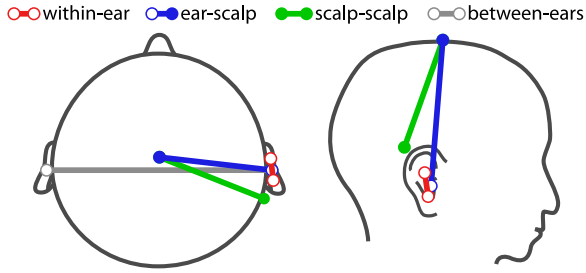


Fig. 4. Illustration of the electrode configurations used in the data analysis. Filled circles indicate wet scalp electrodes and open circles indicate dry-contact ear-electrodes.

### C. Experimental Setup

The dry-contact ear-EEG platform was tested in an EEG study of 12 subjects. The EEG recordings were acquired with a sampling rate of 500 Hz by a 32 channel portable TMSi MOBITA EEG amplifier (TMSi, The Nederlands). The amplifier was characterized by a high input impedance (>4 GΩ) and low noise ($< 0.4\ \mu$V @ 0.1 to 10 Hz). In addition, the amplifier enabled active shielding (guarding) of the ear-electrodes all the way to the backside of each of the 12 electrodes. An easycap (Easycap, Germany) containing 20 wet $IrO_2$ electrodes were used for scalp recordings, as shown in Fig. 3. The scalp electrodes were positioned according to the 10–20 system [22]. A conductive bracelet on the right arm was connected to the GND of the EEG amplifier. Prior to insertion of the earpieces, the ears were cleaned with alcohol and water.

12 subjects with normal hearing and vision aged on average 30.9 (s.d. 5.6) years, participated in the study. The recordings were performed in a laboratory, where the subjects were seated in a comfortable chair and instructed to relax.

The stimulus for a steady-state visual evoked potential (SSVEP) was given by modified active shutter glasses (SSVEP glasses), as shown in Fig. 3(b). The electronics in the glasses were removed and wires were connected directly to the LCD panel, covering the lenses of the glasses. Thereby it was possible to modulate the ambient light. The modulation was controlled by a 5 V 50% duty cycle signal. The rise and fall time of the modulation were 20 $\mu$s and 1000 $\mu$s, respectively.

For auditory paradigms, the stimuli were presented to the subjects with equal phase and intensity in both ears by insert earphones (3M E-A-RTONE GOLD). The tubes from the earphones were inserted into the vents of the earpieces. The stimuli were presented at a sound level of 55 dB above the individual auditory sensation level, determined at 1000 Hz. During the auditory stimulation, the subjects were watching a silent movie without subtitles.

All recordings were bandpass filtered with the EEGLAB FIR filter function "pop_eegfiltnew()" [23]. The cutoff frequencies of the filter are specified below for each paradigm.

### D. Electrode Configurations

To show how the studied responses changed with the location of the electrodes, the data were analyzed with the electrode configurations illustrated in Fig. 4. Within-ear: The measuring electrode and the reference electrode were located within the same ear. Ear-scalp: The measuring electrode was an ear-electrode and the reference was the Cz scalp electrode. Scalp-scalp: The measuring electrode was the TP7 or TP8 electrode and the reference was the Cz electrode. Between-ears: The measuring electrode and the reference electrode were located in the ears on either side of the head.

### E. Discarding of Ear-Electrodes

Discarding of ear-electrodes were based on statistical significance of a 40 Hz auditory steady-state response (ASSR). The ASSR was calculated for all possible within-ear electrode configurations, and electrodes were discarded if they were not involved in an electrode configuration with a statistically significant ASSR (F-test, $p < 0.05$). More specifically, the data were bandpass filtered from 2 to 100 Hz and segmented in 1 s segments. To remove epochs with a high artifact level, the 256 segments with the lowest mean power from 55 to 75 Hz were selected, for each electrode configuration. The ASSR was extracted by time-domain averaging (TDA) of the segments, and the SNR was calculated as the ratio between the power of the first harmonic ASSR (at 40 Hz), and the mean power from 35 to 45 Hz (40 Hz excluded).

### F. Steady-State Responses

Two steady-state stimuli were studied. Each of the stimuli was presented to the subjects for 5 minutes.

The ASSR stimulus was Gaussian distributed white noise amplitude modulated with 40 Hz (Modulation depth of 100%).

The SSVEP stimulation was performed by modulating the ambient light with 9 Hz by using the SSVEP glasses presented above. The subjects were seated in front of a 40" monitor displaying a white screen. The distance from the forehead to the monitor was approximately 60 cm.

The recordings were bandpass filtered to retain frequencies between 2 and 100 Hz, and a second order 50 Hz notch filter was applied to reduce power line interference. Then, the data were segmented in 1 s segments. To ensure coherent averaging of the steady-state responses (SSRs), the segments were aligned to 8 Hz triggers for the ASSR and 9 Hz triggers for the SSVEP. To calculate the SSR for ear-scalp and scalp-scalp electrode configurations, the 256 segments with the lowest mean power from 55 to 75 Hz were selected, and TDA of the segments were performed.

The measured potential difference generally depends on the electrode distance and the orientation of the electrodes relative to the gradient of the potential field [24]. Thus, for within-ear electrode configurations, the electrode distances will be smaller, and consequently the SSR amplitude will generally be lower, when compared to ear-scalp electrode configurations [12], [21]. Moreover, due to individual differences in the anatomical shape of the ear and in the location and orientation of the underlying neural sources, the optimal within-ear electrode configurations will be different across subjects [25]. Therefore, the optimal within-ear electrode configurations were selected individually for each subject. To avoid over-fitting, each configuration was trained on half of the extracted segments, and tested on the other half of the segments. This cross-validation was performed for 100 different training and test configurations, and the TDA of all the test data was calculated. Specifically, for each cross-validation, the training was performed with 128 segments randomly selected from the 256 segments with the lowest mean power from 55 to 75 Hz. Then, the within-ear electrode configuration resulting in the highest SNR of the first harmonic SSR was selected. Testing was performed with the selected electrode configuration and the remaining 128 segments. The SSR was calculated as the TDA of the test data from the 100 cross-validations.

The SNR is defined as the ratio between the power of the signal and the power of the noise. The SNR was calculated at each of the harmonics of the SSR as the power at the harmonic, divided by the power of the noise in a frequency band $\pm 5$ Hz relative to the harmonic. The power at the harmonic was excluded from the noise power estimate.

### G. Mismatch Negativity

The standard stimuli were a 1 kHz sinusoid of duration 75 ms (including 5 ms rise and fall times). The deviant stimuli were deviating in frequency (2 kHz) and randomly selected with a probability of 0.2. The stimulus-onset asynchrony (SOA) was randomly chosen between 500 and 800 ms. A total of 2000 stimuli (400 deviants) were presented in two 11 minutes sequences.

The recorded EEG data were bandpass filtered from 1 to 25 Hz and segmented with limits of $-100$ to 500 ms relative to the onset of the stimulus. Then, each segment was baseline corrected by the mean amplitude from $-100$ to 0 ms, and subsequently segments with amplitudes outside the limits of $\pm 50$ $\mu$V were discarded. The noise level of each segment was estimated as the mean power from 55 to 75 Hz, based on the unfiltered EEG data. The 256 standard stimulus segments with the lowest noise level were selected from each of the two sequences, and the standard event related potential (ERP) was calculated by TDA of these 512 segments. Similarly, the 128 deviant stimulus segments with the lowest noise level were selected from each of the two sequences, and the deviant ERP was calculated by TDA of these 256 segments.

### H. Alpha-Band Modulation

To complement the steady-state and event-related responses, the study also comprised recordings of spontaneous EEG. The study focused on alpha-band activity, which is modulated by visual attention. The subjects were instructed for two conditions; 1) Eyes open, watching the silent movie. 2) Relaxing with closed eyes. An auditory cue indicated a change in condition every 60 s. The first condition was always condition 1. The measurement had a duration of 4 minutes.

The EEG data were bandpass filtered from 2 to 45 Hz and segmented in 4 s segments, with 2 s overlap. For each segment, the mean alpha-band power (8 to 12 Hz) was calculated. Segments with a mean alpha-band power above 100 $\mu V^2/Hz$ for ear-scalp electrode configurations and 1 $\mu V^2/Hz$ for within-ear electrode configurations were left out of the analysis.

The primary alpha sources during closed eyes are occipital, and thus not within close proximity of the ear [26]. Considering the small electrode distances within the ear, it was necessary to optimize the within-ear electrode configuration for each subject. The data were divided into two data sequences, with the first data sequence containing the first 120 s of the EEG data and the second data sequence containing the remaining 120 s. Then, the within-ear electrode configuration resulting in the highest alpha-band modulation ratio, was selected for each data sequence. To avoid overfitting, the selected electrode configuration was used for the analysis of the EEG data in the opposite data sequence.

### I. Electrode-Skin Impedance

To obtain a better understanding of the electrode-skin interface for the developed dry-contact ear-EEG platform, characterization of the electrode-skin impedance spectrum was performed for all subjects. Impedance spectra were measured for all 12 ear-electrodes in the end of the study, at which point the subjects had been wearing the earpieces for approximately 2 hours.

The electrode-skin impedance for wet and dry-contact ear-EEG electrodes have previously been characterized for silver (Ag) electrodes in [6]. The study described equipment to measure the impedance spectrum, and presented measurements of the impedance spectrum for the Ag electrodes. The same equipment was used to characterize the electrode-skin impedance for the developed $IrO_2$ dry-contact electrode.

The impedance measurements were performed with a current density of 0.5 $\mu A/cm^2$, and the impedance spectrum was measured for 10 combinations of the 6 electrodes in each ear. This enabled a robust estimation of the electrode-skin impedance for a single electrode (single electrode-skin interface). 6 of the impedance measurements, for each ear, were performed between an ear-electrode and a conductive bracelet on the left arm. The GND of the impedance setup was always connected to a conductive bracelet on the right arm. The impedance spectra and parameters for an electrical model of the electrode-skin interface were estimated as described in [6].

### J. Half-Cell Potential

The half-cell potential was measured for 5 electrodes, which were constructed in such way that only the $IrO_2$ coating was exposed. All measurements were performed relative to a SI Analytics 2820+[2] reference electrode (Xylem Analytics, Germany). The electrodes were submerged in a container with 1Mol KCl at temperature 25 °C, and measurements were performed

[2]Ag/AgCl electrode in a 3Mol KCl solution, cheramic membrane.

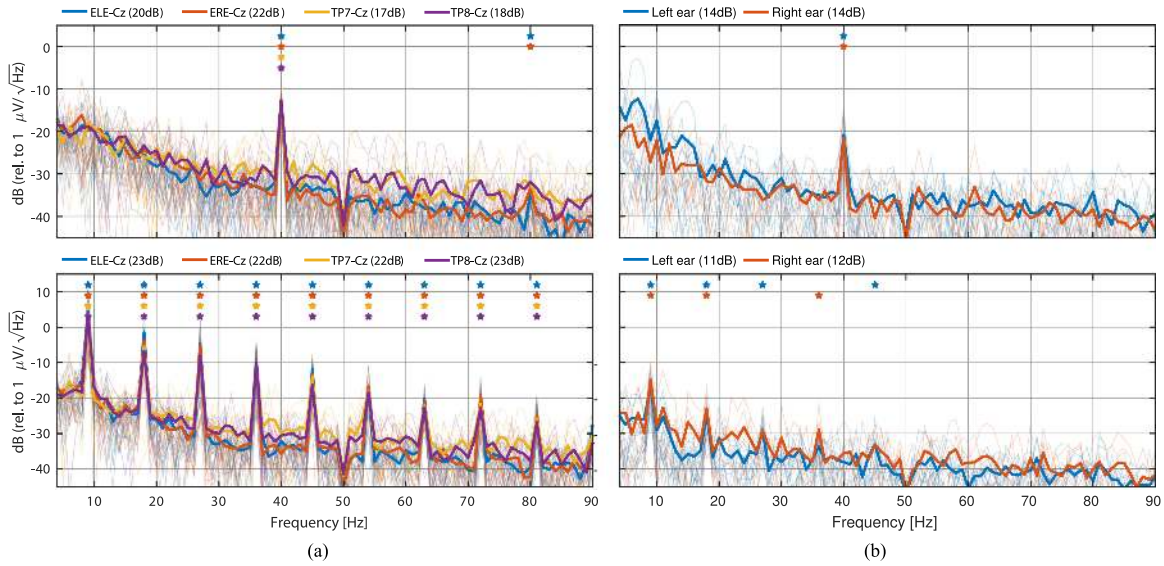


Fig. 5. Grand average power spectra of the ASSR (top row) and SSVEP (bottom row). (a) Ear-scalp and scalp-scalp electrode configurations. (b) Within-ear electrode configurations. The faded lines are the response for each subject. The SNR of the first harmonic response is given in the legends, and a star marker indicate a statistically significant ($p < 0.05$) response, based on a F-test.

TABLE I
DISCARD RATIOS FOR THE DATA ANALYSIS, GIVEN FOR EACH EAR-ELECTRODE LOCATION

| Left ear | | | | | | Right ear | | | | | |
|---|---|---|---|---|---|---|---|---|---|---|---|
| ELA | ELB | ELC | ELE | ELI | ELT | ERA | ERB | ERC | ERE | ERI | ERT |
| 0.3 | 0.2 | 0.3 | 0.2 | 0.3 | 0.1 | 0.0 | 0.2 | 0.3 | 0.1 | 0.0 | 0.1 |

Concha electrodes marked with gray.

with a HMC 8012 multimeter[3] (Rohde & Schwartz, Germany). The measured potentials were subtracted 27.7 mV, according to Nernst equation, to correct for the different KCl solutions in the container and reference electrode.

For each measurement, the electrode was submerged in the container, 20 minutes later the half-cell potential was measured, and the electrode was removed and cleaned with water. This procedure was repeated 4 times for each electrode.

## III. RESULTS

In the following we present EEG recordings performed with the developed dry-contact ear-EEG platform and wet scalp electrodes. According to the discard criteria, a few recordings from the ear-electrodes were discarded as given in Table I.

### A. Steady-State Responses

The top row of Fig. 5 shows grand average ASSRs and the bottom row shows grand average SSVEPs. Power spectra for ear-scalp and scalp-scalp electrode configurations are shown in Fig. 5(a) (left column), and Fig. 5(b) (right column) shows power spectra for within-ear electrode configurations, which was optimized for each subject, as described above. The SNRs of the first harmonic responses are given in the legends, and star markers indicate statistically significant responses (F-test, $p < 0.05$). The figure shows similar ASSRs and SSVEPs for the ear-scalp and scalp-scalp electrode configurations. Comparing the power spectra for the ear-scalp and within-ear electrode configurations, the SNR values were lower for the within-ear electrode configurations, but the first harmonic responses were still easily observable and statistically significant. The noise floor of the power spectra, was comparable for the within-ear and ear-scalp electrode configurations.

[3]Input impedance $>10$ GΩ.

### B. Mismatch Negativity

Fig. 6(a) shows the grand average MMN response for the ear-scalp electrode configuration ELE-Cz. Fig. 6(b) shows the grand average MMN response for the electrode configuration TP7-TP8, and Fig. 6(c) shows the response for the between-ears electrode configuration ELE-ERE. The green line color indicate intervals where the MMN response was statistically significant ($p < 0.05$, no multiple comparison correction) different from zero, measured by a one sample t-test. Both the standard and deviant ERP, for the ELE-Cz configuration, had the well-known P1-N1-P2 waveform, with timing and amplitudes similar to previous wet electrode ear-EEG recordings [13]. The timing of the MMN response changed slightly when the electrode configuration was changed from the ELE-Cz to the ELE-ERE. However, the timing of the MMN response was similar for the TP7-TP8 and the ELE-ERE electrode configurations. General for all the electrode configurations in Fig. 6, the MMN response was statistically significant for continuous intervals at the time of the most prominent peaks. The MMN response is only shown for a between-ears electrode configuration as it was not statistically significant for within-ear electrode configurations.

### C. Alpha-Band Modulation

Fig. 7 shows spectrograms with corresponding power spectra for recordings from a single subject. The plot below each spectrogram shows the grand average of the mean alpha-band power, 8 to 12 Hz. For the calculation of the grand average mean

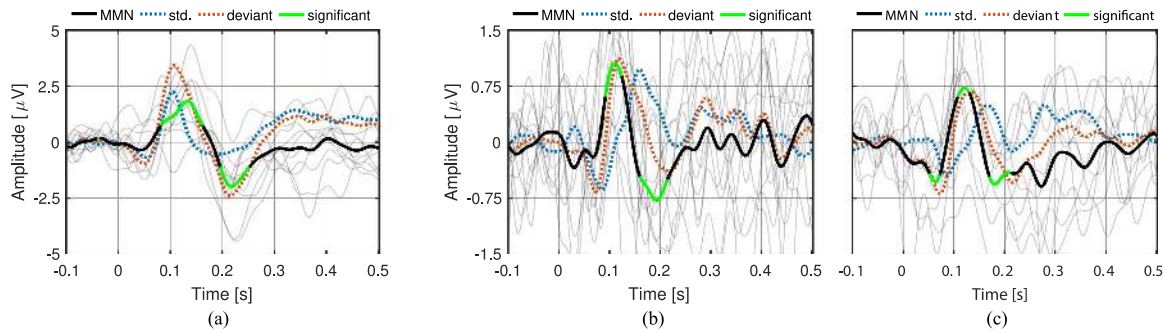


Fig. 6. Grand averaged MMN responses. (a) Ear-scalp configuration ELE-Cz. (b) Electrode configuration TP7-TP8. (c) Between-ears configuration ELE-ERE. The faded lines are the MMN response for each subject. The green line intervals indicate a grand averaged MMN response statistically significant ($p < 0.05$, no multiple comparison correction) different from zero, measured by a one sample t-test.

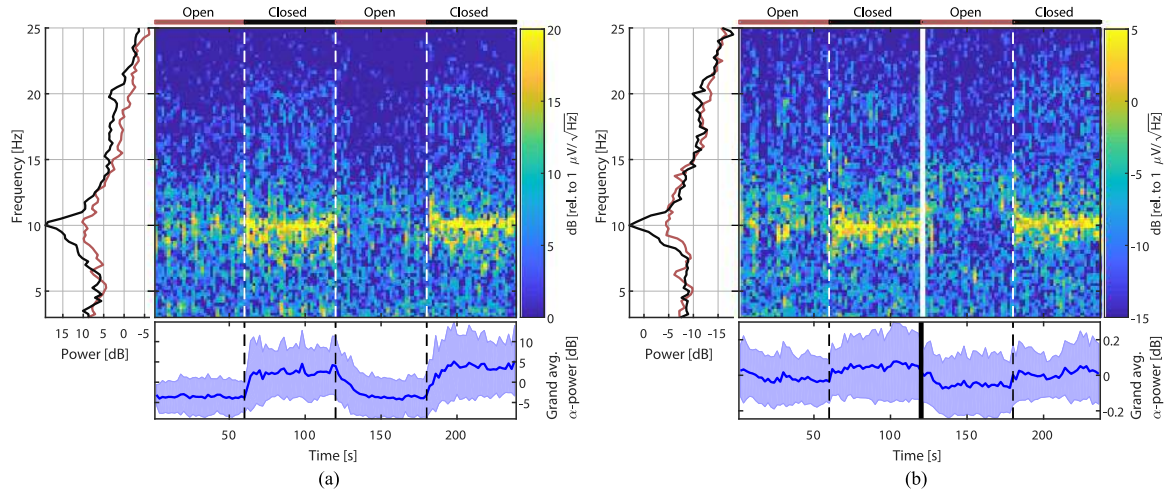


Fig. 7. Top: Power spectrum and spectrogram for subject 11 with indication of open and closed eyes intervals. Bottom: Grand average of the mean alpha-band power (8 to 12 Hz). (a) Ear-scalp electrode configuration ELE-Cz. (b) Within-ear electrode configuration. The shaded area indicate plus/minus one standard deviation (s.d.) of the grand average. The grand average plots have been smoothed with a 3 tap mean filter. All dB values are relative to $1\ \mu\text{V}/\sqrt{\text{Hz}}$.

alpha-band power, 1% of the segments for the ELE-Cz electrode configuration and 14% of the segments for the within-ear electrode configuration were discarded, according to the criteria described above.

The spectrogram and plot of the grand average alpha-band power, for the ELE-Cz electrode configuration, show a clear and statistically significant ($p < 0.001$) alpha-band modulation. The alpha-band modulation, for the within-ear electrode configuration, was lower, but the grand average modulation was still statistically significant ($p < 0.001$). According to Table II, the alpha-band modulation was statistically significant ($p < 0.05$) for 9 out of 10 subjects with the ELE-Cz electrode configuration, and 5 out of 12 subjects with the within-ear electrode configuration.

TABLE II
ALPHA-BAND MODULATION RATIO FOR CLOSED/OPEN EYES, AND CORRESPONDING P-VALUES FOR AN UNPAIRED T-TEST

| | **ELE-Cz** | | **Within-ear** | |
|---|---|---|---|---|
| Subject | $\alpha$ mod. | p | $\alpha$ mod. | p |
| 1 | 3.6 | <0.001 | 1.1 | 0.016 |
| 2 | - | - | 1.1 | 0.412 |
| 3 | 2.1 | <0.001 | 1.2 | 0.060 |
| 4 | 1.1 | 0.705 | 1.8 | 0.220 |
| 5 | 3.1 | <0.001 | 0.9 | 0.160 |
| 6 | 2.4 | <0.001 | 1.5 | <0.001 |
| 7 | 1.5 | <0.001 | 0.8 | 0.126 |
| 8 | 6.6 | <0.001 | 1.4 | 0.021 |
| 9 | 2.6 | <0.001 | 1.9 | <0.001 |
| 10 | 1.9 | <0.001 | 1.1 | 0.296 |
| 11 | 3.7 | <0.001 | 2.4 | <0.001 |
| 12 | - | - | 1.1 | 0.725 |
| Grand avg. | 2.7 | <0.001 | 1.2 | <0.001 |

"-" indicates discarded recordings.

## D. Electrode-Skin Impedance

Fig. 8(a) shows grand averaged model parameters for electrodes in the ear-canal. The model parameters are based on measurements from wet and dry-contact silver (Ag) electrodes on rigid earpieces and dry-contact $IrO_2$ electrodes mounted in soft-earpieces. The parameters for the Ag electrodes are taken from [6]. The resistance and capacitance were comparable for the dry Ag and dry $IrO_2$ electrodes, with R1 dominating the

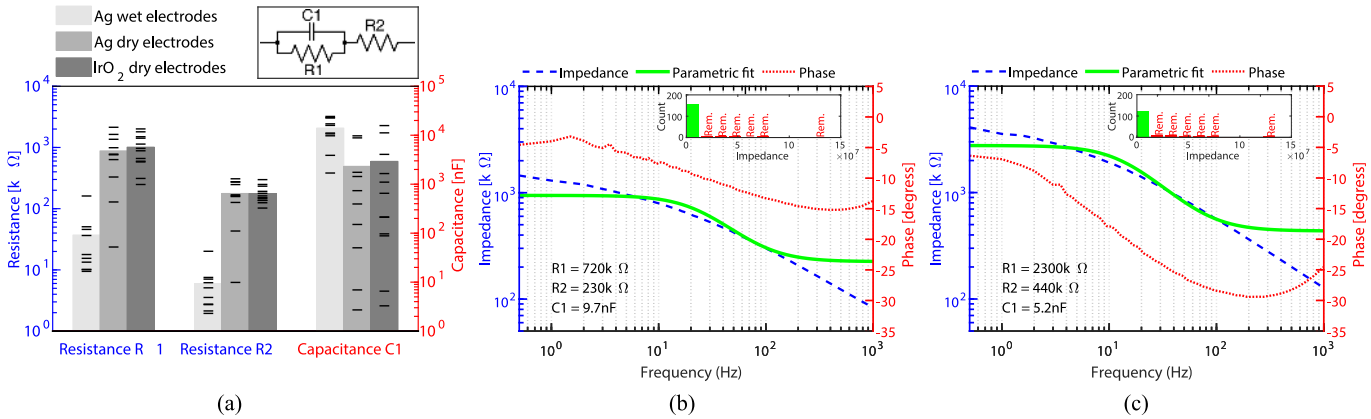


Fig. 8. (a) Comparison of parameter values for the electrode-skin interface of electrodes in the ear-canal. The parametric model is shown in the legend. The black lines indicate parameter values for single recordings. (b) Impedance spectrum for dry-contact $IrO_2$ electrodes in the ear-canal. (c) Impedance spectrum for dry-contact $IrO_2$ electrodes in the concha. (b) & (c) The histogram in the upper right corner shows the distribution of the mean impedance from 0.1 Hz to 10 Hz. A few recordings, marked by "Rem.", were outliers in the histogram and left out of the analysis. All impedance measurements were performed with the earpieces inserted into the ears of the subjects.

resistive part of the electrode-skin interface. For comparison, the impedance at approximately 50 Hz for ear-canal electrodes were: 4 kΩ (s.d. 3 kΩ) for wet Ag, 452 kΩ (s.d. 737 kΩ) for dry Ag, and 435 kΩ (s.d. 515 kΩ) for dry $IrO_2$.

Fig. 8(b) and (c) show grand average impedance spectra for the dry $IrO_2$ electrodes in the ear-canal and concha, respectively. The histogram in the upper right corner of Fig. 8(b) and (c) displays the distribution of the mean impedance from 0.1 Hz to 10 Hz. A few measurements, marked by "Rem.", were outliers in the histogram and left out of the analysis. In total, measurements from 12 (7.1%) electrodes were left out of the analysis.

### E. Half-Cell Potential

The half-cell potential was measured to an average of 99 mV (s.d. 29 mV), corresponding to a half-cell potential of 322 mV when referenced to the standard hydrogen electrode.

Measurements of the half-cell potential were performed in an electrolyte solution (1M KCl), and did not resemble dry skin contact. To supplement the half-cell potential measurements and to obtain an estimate of the offset tolerance required to measure with the developed electrode on skin, the DC offset was calculated for all the included ASSR recordings. The calculations were performed for ear-electrodes in both ears, and with average reference. The standard deviation of the offset for 122 measurements was 46 mV (min = −108 mV, max = 176 mV).

## IV. Discussion

### A. Steady-State Responses

The high similarity between the ASSRs and SSVEPs for the scalp-scalp and ear-scalp electrode configurations shows that the dry-contact ear-electrodes measured meaningful EEG signals, and that the quality of the recordings were on par with recordings from conventional wet scalp electrode setups. When the electrode configurations were changed from ear-scalp to within-ear, the amplitude of the first harmonic ASSRs decreased approximately 10 dB. This decrease is smaller, but still comparable to previous ear-EEG recordings based on wet electrodes [12], [13], and is primarily caused by the smaller electrode distances. However, the SNR of the ASSR decreased with 6–8 dB from the ear-scalp to the within-ear electrode configurations. This is not consistent with previously reported results, where the SNR was similar or higher for within-ear electrode configurations [12], [21], [27]. The decreased SNR was caused by a similar noise floor of the power spectra for the ear-scalp and within-ear electrode configurations. This was most likely related to increased noise in the electrode-skin interface of the dry-contact electrodes compared to the wet scalp electrodes.

The first 8 harmonics of the SSVEP were statistically significant for both the scalp-scalp and ear-scalp electrode configurations. However, for the within-ear electrode configurations only the first two harmonics were consistently statistically significant. The amplitude of the SSVEPs were approximately 20 dB lower for the within-ear electrode configurations compared to the ear-scalp electrode configurations. This is largely consistent with previously reported results for wet ear-electrodes [12]. The SNR of the SSVEP decreased 10–12 dB from the ear-scalp to the within-ear electrode configurations. As for the ASSR results, this was mainly due to a lower amplitude of the SSVEP, while the noise floor of the power spectra for the ear-scalp and within-ear electrode configurations were similar.

### B. Mismatch Negativity

The MMN response for the ear-scalp electrode configuration ELE-Cz had timing of the peaks which corresponded to previous studies of MMN, where the electrode configuration and paradigm were similar [28]. The first peak of the MMN response was elicited around 150 ms, which is consistent with [29].

When the electrode configuration was changed to TP7-TP8 and ELE-ERE, the amplitude of the MMN response was lower and the timing of the peaks was slightly changed. This is likely a consequence of the changed electrode configuration, which results in a different weighting of the neural sources related to the MMN response. The significant points constituted continuous intervals around the most prominent peaks, which suggests that

these intervals were significant and not just random variations in the statistical test.

### C. Alpha-Band Modulation

Fig. 7(a) shows a clear grand average alpha-band modulation for the ear-scalp electrode configuration ELE-Cz. When the electrode configuration was changed to within-ear, the grand average alpha-band modulation was less visible, but still statistically significant. Compared to previous studies of alpha-band modulation performed with wet ear-electrodes, the modulation for a within-ear electrode configuration was lower in the current study [21]. The lower modulation was probably related to a higher noise level of the dry-contact electrode recordings, which was also observed for the SSR recordings. However, Fig. 7 clearly shows that alpha-band modulation can be measured with the developed dry-contact ear-EEG platform.

### D. Electrode-Skin Impedance

The model parameters for dry Ag and dry $IrO_2$ electrodes were comparable, even though the electrode area of the $IrO_2$ electrodes were approximately 1.5 times smaller than the area of the dry Ag electrodes. In addition, the Ag electrodes were painted on the surface of individualized rigid earpieces, and therefore they most likely had a better fit with the ear-canal. The developed $IrO_2$ electrode had a fixed shape, which might have caused the skin contact area to be smaller than the electrode surface area. Thus, the ratio between the contact area of the Ag and $IrO_2$ electrodes might be larger than 1.5.

The double-layer of the electrode-skin interface was modeled by C1 and R1, and R2 modeled the ohmic resistance of the electrolyte, skin, and bulk tissue [7]. For dry-contact electrodes, the formation of a double layer is limited by the amount of moisture, from the body, condensed on the surface of the electrode. This cause the impedance of the double-layer to increase, compared to wet electrodes. This could explain why R1 was dominating the resistive part of the electrode-skin interface for the dry-contact electrode measurements.

In [6] impedance measurements for dry Ag electrodes located in the concha region of the ear were not included, due to extreme impedances for these electrodes. The current study illustrates that with soft-earpieces and $IrO_2$ electrodes, it is possible to obtain an acceptable electrode-skin impedance for dry-contact electrodes in the concha. However, the impedance for the concha electrodes were higher than the impedance for the ear-canal electrodes. This is in accordance with our practical experience, which have showed that it is more difficult to achieve a good electrode-skin interface in the concha region. In a previous study of physiological artifacts in ear-EEG [21], we speculated that soft-earpieces could be an improvement over rigid earpieces. The impedance measurements for the concha electrodes further consolidate this speculation.

The developed dry-contact electrodes had electrode-skin impedances approximately two orders of magnitude higher than comparable wet electrodes. This should be taken into consideration when designing an instrumentation amplifier for measuring with the electrodes. Electrode impedance imbalances generally scale with the absolute value of the impedance. Thus, the impedance imbalances are also expected to be two orders of magnitude higher for the developed dry-contact electrodes compared to wet electrodes. The common mode rejection ratio (CMRR) of an instrumentation amplifier is limited by $\mathrm{CMRR_{elec}} \cong 20 \cdot \log_{10}\left(\frac{Z_C}{\Delta Z_E}\right)$, where $\Delta Z_E$ is the impedance imbalance and $Z_C$ is the common mode input impedance of the instrumentation amplifier [6], [7]. Consequently, the input impedance of the instrumentation amplifier must be two orders of magnitude higher to achieve the same CMRR for dry-contact electrodes as for wet electrodes. Regarding the input referred noise, the main focus should be on the current noise, because the current noise is multiplied by the electrode-skin impedance; $n_{input} = v_n + Z_E \cdot i_n$, where $n_{input}$ is the total input referred noise, $v_n$ is the input referred voltage noise, and $i_n$ is the input referred current noise. Thus, all other things being equal, the input referred current noise of the instrumentation amplifier must be two orders of magnitude lower to achieve the same input referred noise level for dry-contact electrodes as for wet electrodes.

### E. Half-Cell Potential

The measurements of the half-cell potential had a standard deviation of 29 mV across 5 electrodes and 4 repeated measurements. This shows a reasonably low variation across electrodes and repetitions. In addition, calculations of the required offset tolerance showed that an instrumentation amplifier with an offset tolerance of at least $+/-92$ mV ($\pm 2$ s.d.) is necessary to obtain reliable recordings with the developed dry-contact ear-EEG platform.

### F. Towards Real-Life Long-Term Recordings

While it is a clear objective to develop a wearable ear-EEG device for long-term brain monitoring in real-life, the technology is not presently at a stage where this is possible. The current study is one of the necessary steps towards this goal and demonstrates that dry-contact ear-EEG recordings can be performed under well controlled laboratory conditions.

For long-term real-life ear-EEG recordings to be feasible, a compact ear-EEG platform with high comfort must be available. Steps towards the development of a compact ear-EEG platform was taken in [30], where we presented a low power application-specific integrated circuit (ASIC) for measuring ear-EEG. However, the current version of the ASIC is not easily implemented in a portable and compact system, and further development is needed to reach this goal. The soft-earpieces, introduced in the current paper, are commonly used for hearing aids, and are known to be comfortable for long-term use. To obtain good and reproducible recording conditions, the ears were cleaned with alcohol prior to the insertion of the earpieces. However, this procedure would not be comfortable and feasible for long-term use, and does not comply with everyday use. Future studies should investigate the relation between recording quality and the degree of cleaning. The durability of the electrodes is also an important aspect when performing long-term recordings. Considering the inert nature of the $IrO_2$ coating and the results of the biocompatibility test, the developed platform is expected to sustain long-term exposure to perspiration, ear wax, and everyday

environments. From a user perspective, the device should be easy to insert into the ear, and the recording quality should be stable over several insertions and days. The laboratory setup for the current study did not allow the subjects to insert the earpieces themselves. However, for everyday use, the subject should insert the earpieces at home, and, in that context, a usability study would be relevant to cover reproducibility of recordings over several insertions and days. Moreover, to improve the usability for long-term real-life recordings, the GND-electrode should be moved to the earpiece.

## V. Conclusion

A novel dry-contact ear-EEG platform, comprising actively shielded and nano-structured electrodes embedded in an individualized soft-earpiece, was developed and prototyped. The platform was evaluated in a study of 12 subjects and four EEG paradigms: auditory steady-state response (ASSR), steady-state visual evoked potential (SSVEP), mismatch negativity (MMN), and alpha-band modulation. The measurements were analyzed with 4 electrode configurations: 1) Within-ear: measuring electrode and reference electrode within the same ear. 2) Ear-scalp: measuring electrode in the ear and reference at the Cz scalp location. 3) Scalp-scalp: measuring electrode close to the ear and reference at the Cz location. 4) Between-ears: measuring electrode and reference electrode located in opposite ears. Ear-scalp measurements of the ASSR and SSVEP were on par with scalp-scalp measurements. Changing to the within-ear configuration resulted in decreased response amplitudes, which is consistent with previous studies. Unfortunately, the noise floor did not decrease correspondingly, resulting in lower signal-to-noise ratios (SNRs). Despite the lower SNRs, the responses were clearly observable and statistically significant ($p < 0.05$). The MMN waveform and timing in ear-scalp measurements corresponded well with literature. The MMN were observable and statistically significant in between-ears measurements, whereas no MMN was observed in within-ear measurements. Alpha-band modulation related to open/closed eyes was clear and statistically significant in ear-scalp measurements. The modulation was lower but statistically significant for within-ear measurements. Electrode-skin impedance spectra were also measured for all subjects, and showed that it was more difficult to achieve a good electrode contact in the concha region compared to the ear-canal, which is in accordance with our practical experience. Based on the study, it is concluded that dry-contact electrode ear-EEG is a feasible technology for EEG recordings. We believe that the prototyped dry-contact ear-EEG platform represents an important technological advancement in user-friendliness, because it eliminates the need for gel in the electrode-skin interface.

## References


[1] A. J. Casson *et al.*, "Wearable electroencephalography," *IEEE Eng. Med. Biol. Mag.*, vol. 29, no. 3, pp. 44–56, May/Jun. 2010.

[2] S. Debener *et al.*, "Unobtrusive ambulatory EEG using a smartphone and flexible printed electrodes around the ear," *Sci. Rep.*, vol. 5, Nov. 2015, Art. no. 16743.

[3] J. H. Lee *et al.*, "CNT/PDMS-based canal-typed ear electrodes for inconspicuous EEG recording," *J. Neural Eng.*, vol. 11, no. 4, Jun. 2014, Art. no. 046014.

[4] J. J. S. Norton *et al.*, "Soft, curved electrode systems capable of integration on the auricle as a persistent brain–computer interface," *Proc. Nat. Acad. Sci. USA*, vol. 112, no. 13, pp. 3920–3925, Mar. 2015.

[5] D. Looney *et al.*, "An In-the-ear platform for recording electroencephalogram," in *Proc. Conf. IEEE Eng. Med. Biol. Soc.*, 2011, pp. 6882–6885.

[6] S. L. Kappel and P. Kidmose, "Study of impedance spectra for dry and wet EarEEG electrodes," in *Proc. Conf. IEEE Eng. Med. Biol. Soc.*, 2015, pp. 3161–3164.

[7] Y. M. Chi, T. P. Jung, and G. Cauwenberghs, "Dry-Contact and noncontact biopotential electrodes: Methodological review," *IEEE Rev. Biomed. Eng.*, vol. 3, pp. 106–119, Oct. 2010.

[8] P. Fiedler *et al.*, "Novel multipin electrode cap system for dry electroencephalography," *Brain Topography*, vol. 28, no. 5, pp. 647–656, Sep. 2015.

[9] C. T. Lin *et al.*, "Novel dry polymer foam electrodes for long-term EEG measurement," *IEEE Trans. Biomed. Eng.*, vol. 58, no. 5, pp. 1200–1207, May 2011.

[10] P. Fiedler *et al.*, "Multichannel EEG with novel Ti/TiN dry electrodes," *Sens. Actuators A: Phys.*, vol. 221, no. 1, pp. 139–147, Jan. 2015.

[11] Y. M. Chi *et al.*, "Dry and noncontact EEG sensors for mobile brain-computer interfaces," *IEEE Trans. Neural Syst. Rehabil. Eng.*, vol. 20, no. 2, pp. 228–235, Mar. 2012.

[12] P. Kidmose *et al.*, "A study of evoked potentials from Ear-EEG," *IEEE Trans. Biomed. Eng.*, vol. 60, no. 10, pp. 2824–2830, Oct. 2013.

[13] K. B. Mikkelsen *et al.*, "EEG recorded from the Ear: Characterizing the Ear-EEG method," *Front. Neurosci.*, vol. 9, Nov. 2015, Art. no. 438.

[14] M. G. Bleichner *et al.*, "Exploring miniaturized EEG electrodes for brain-computer interfaces. An EEG you do not see?" *Physiol. Rep.*, vol. 3, no. 4, Apr. 2015, Art. no. e12362.

[15] S. L. Kappel *et al.*, "A method for quantitative assessment of artifacts in EEG, and an empirical study of artifacts," in *Proc. Conf. IEEE Eng. Med. Biol. Soc.*, 2014, pp. 1686–1690.

[16] R. D. Meyer *et al.*, "Electrodeposited iridium oxide for neural stimulation and recordingelectrodes," *IEEE Trans. Neural Syst. Rehabil. Eng.*, vol. 9, no. 1, pp. 2–11, Mar. 2001.

[17] S. F. Cogan, "Neural stimulation and recording electrodes," *Annu. Rev. Biomed. Eng.*, vol. 10, pp. 275–309, Aug. 2008.

[18] N. S. Dias *et al.*, "New dry electrodes based on iridium oxide (IrO) for non-invasive biopotential recordings and stimulation," *Sens. Actuators A: Phys.*, vol. 164, nos. 1/2, pp. 28–34, Nov./Dec. 2010.

[19] J. Augustynski *et al.*, "ESCA study of the state of iridium and oxygen in electrochemically and thermally formed iridium oxide films," *J. Electroanal. Chem. Interfacial Electrochem.*, vol. 160, nos. 1/2, pp. 233–248, Jan. 1984.

[20] S. A. M. Marzouk, "Improved electrodeposited iridium oxide pH sensor fabricated on etched titanium substrates," *Anal. Chem.*, vol. 75, no. 6, pp. 1258–1266, Mar. 2003.

[21] S. L. Kappel *et al.*, "Physiological artifacts in scalp eeg and ear-eeg," *Biomed. Eng. Online*, vol. 16, no. 1, Aug. 2017, Art. no. 103.

[22] H. H. Jasper, "Report of the committee on methods of clinical examination in electroencephalography," *Electroencephalography Clin. Neurophysiol.*, vol. 10, pp. 370–375, 1958.

[23] A. Delorme and S. Makeig, "EEGLAB: An open source toolbox for analysis of single-trial EEG dynamics including independent component analysis," *J. Neurosci. Methods*, vol. 134, no. 1, pp. 9–21, Mar. 2004.

[24] S. L. Kappel and P. Kidmose, "High-density ear-eeg," in *Proc. Conf. IEEE Eng. Med. Biol. Soc.*, 2017, pp. 2394–2397.

[25] S. L. Kappel *et al.*, "Reference configurations for Ear-EEG steady-state responses," in *Proc. Conf. IEEE Eng. Med. Biol. Soc.*, 2016, pp. 5689–5692.

[26] O. N. Markand, "Alpha rhythms," *J. Clin. Neurophysiol.*, vol. 7, no. 2, pp. 163–189, 1990.

[27] C. B. Christensen *et al.*, "Ear-EEG based objective hearing threshold estimation evaluated on normal hearing subjects," *IEEE Trans. Biomed. Eng.*, vol. 65, no. 5, pp. 1026–1034, May 2018.

[28] R. Näätänen and R. Takegata, "The Mismatch Negativity (MMN)," in *The Oxford Handbook of Event-Related Potential Components*, 1st ed., S. J. Luck and E. S. Kappenman, Eds. Oxford, U.K.: Oxford Univ. Press, 2011, ch. 6, pp. 143–157.

[29] R. Näätänen *et al.*, "The mismatch negativity (MMN): Towards the optimal paradigm," *Clin. Neurophysiol.*, vol. 115, no. 1, pp. 140–144, Jan. 2004.

[30] X. Zhou *et al.*, "A wearable Ear-EEG recording system based on dry-contact active electrodes," in *Proc. Symp. VLSI Technol. Circuits*, Jun. 2016, pp. 1–2.